Aspirin Suppresses PGE$_2$ and Activates AMP Kinase to Inhibit Melanoma Cell Motility, Pigmentation, and Selective Tumor Growth *In Vivo*

Dileep Kumar[1], **Hafeez Rahman**[1], **Ethika Tyagi**[1], **Tong Liu**[1], **Chelsea Li**[1], **Ran Lu**[1], **David Lum**[1], **Sheri L. Holmen**[1,2,3], **J. Alan Maschek**[4], **James E. Cox**[4,5], **Matthew W. VanBrocklin**[1,2,3], **Douglas Grossman**[1,2,6]

[1]Huntsman Cancer Institute, University of Utah Health Sciences Center, Salt Lake City, Utah.

[2]Department of Oncological Sciences, University of Utah, Salt Lake City, Utah.

[3]Department of Surgery, University of Utah Health Sciences Center, Salt Lake City, Utah.

[4]Health Science Center Cores, University of Utah Health Sciences Center, Salt Lake City, Utah.

[5]Department of Biochemistry, University of Utah, Salt Lake City, Utah.

[6]Department of Dermatology, University of Utah Health Sciences Center, Salt Lake City, Utah.

Abstract

There are conflicting epidemiologic data on whether chronic aspirin (ASA) use may reduce melanoma risk in humans. Potential anticancer effects of ASA may be mediated by its ability to suppress prostaglandin E$_2$ (PGE$_2$) production and activate 5′-adenosine monophosphate–activated protein kinase (AMPK). We investigated the inhibitory effects of ASA in a panel of melanoma and transformed melanocyte cell lines, and on tumor growth in a preclinical model. ASA and the COX-2 inhibitor celecoxib did not affect melanoma cell viability, but significantly reduced colony formation, cell motility, and pigmentation (melanin production) *in vitro* at concentrations of 1 mmol/L and 20 μmol/L, respectively. ASA-mediated inhibition of cell migration and pigmentation

was rescued by exogenous PGE_2 or Compound C, which inhibits AMPK activation. Levels of tyrosinase, MITF, and p-ERK were unaffected by ASA exposure. Following a single oral dose of 0.4 mg ASA to NOD/SCID mice, salicylate was detected in plasma and skin at 4 hours and PGE_2 levels were reduced up to 24 hours. Some human melanoma tumors xenografted into NOD/SCID mice were sensitive to chronic daily ASA administration, exhibiting reduced growth and proliferation. ASA-treated mice bearing sensitive and resistant tumors exhibited both decreased PGE_2 in plasma and tumors and increased phosphorylated AMPK in tumors. We conclude that ASA inhibits colony formation, cell motility, and pigmentation through suppression of PGE_2 and activation of AMPK and reduces growth of some melanoma tumors *in vivo*. This preclinical model could be used for further tumor and biomarker studies to support future melanoma chemoprevention trials in humans.

Introduction

Aspirin (acetylsalicylic acid, ASA) has long been recognized for its antipyretic and anti-inflammatory activities that have been attributed largely to its ability to inhibit the prostaglandin-endoperoxide synthase, or COX enzymes (1). ASA inhibits COX by acetylating the enzymatic active site, which prevents binding of arachidonic acid (2). Two COX isoforms (COX-1 and COX-2) are responsible for catalyzing conversion of arachidonic acid to prostaglandins (1); whereas COX-1 expression tends to be constitutive, COX-2 is upregulated in inflammation and cancer (3). Selective COX-2 inhibitors (e.g., celecoxib) were developed to target inflammation and pain while not compromising COX-1–mediated activities such as protection of gastric mucosa, but their cardiac toxicity precludes chronic administration for chemoprevention (4). Prostaglandin E_2 (PGE_2) is particularly relevant to carcinogenic progression, being implicated in angiogenesis (5), tumor cell proliferation (6), migration (7), and invasion (8). ASA has also been shown to activate the 5′-adenosine monophosphate–activated protein kinase (AMPK; ref. 9), which has been associated with promotion (10) and inhibition (11) of the mTOR in various malignant cell types.

ASA has demonstrated safety and chemopreventive activity for colon cancer (12), as well gastric (13), breast (14), and prostate cancer (15). The effect of chronic ASA administration on melanoma risk has largely been investigated in retrospective cohort and case–control studies that have yielded inconsistent results (16). Several large prospective studies (17, 18) examining subject-reported ASA use and cancer risk found protective effects for colon and other cancers, but not for melanoma. In contrast, Gamba and colleagues (19) found that regular ASA use was significantly associated with reduced melanoma risk in postmenopausal women. Several preclinical studies have examined ASA-mediated chemoprotection in animal models of melanoma (20–22). PGE_2 may be a reasonable target in melanoma, given the presence of COX-2 in most melanomas but not benign nevi (23), and its association with melanoma progression (24) and poor patient survival (25).

We investigated various inhibitory effects of ASA in a panel of melanoma and melanocyte cell lines, and the role of PGE_2 and AMPK in this context. Moreover, we developed a preclinical model based on daily oral ASA administration to investigate the potential effect in melanoma chemoprevention and treatment.

Materials and Methods

Cell lines and culture

Human melanoma patient-derived xenografts (PDX) were established under protocol #10924, approved by the University of Utah Institutional Review Board (IRB). Melanoma PDX cell lines were propagated in Mel2 medium (26) containing 2% FBS and antibiotics in a humidified incubator at 37°C. The PDX lines MTG2 (HCIMel002) and MTG4 (HCIMel004) express an $NRAS^{Q61R}$ or $BRAF^{V600E}$ mutation, respectively. The MTG5 (HCIMel005) line expresses both $TP53^{R213X}$ and $PDGFR-A^{D846N}$ mutations. A375 and WM3311 human melanoma cells, expressing a $BRAF^{V600E}$ mutation or no known melanoma driver mutations, respectively, and mouse B16-F10 cells were obtained from the ATCC and maintained in DMEM with 5% FBS and antibiotics (culture medium). YUSAC-2 (YU2) human melanoma cells have been described previously (27). Normal human melanocytes were prepared from discarded foreskins under IRB protocol #8476 and propagated as described previously (28). Human melanocyte lines transformed and immortalized by expression of activated c-Met receptor and telomerase (Mel-STM) or SV40ER, $HRAS^{G12V}$ and telomerase (Mel-STR), as described elsewhere (29), were generously provided by Robert Weinberg (Whitehead Institute, Cambridge, MA) and maintained in culture medium.

MTT assays

Cells in 96-well plates were incubated in 90 μL culture medium containing ASA (Sigma, crystalline, purity >99%) or celecoxib (Sigma, purity >98%) for either 24 or 48 hours; then, 10 μL MTT (5 mg/mL stock, Thermo Fisher Scientific) was added at a final concentration of 1.2 mmol/L and cells were returned to the incubator for 4 hours. After removing the medium, 120 μL of DMSO was added to each well and mixed thoroughly by pipetting, and the plate was then gently shaken in the dark for 20 to 30 minutes. Absorbance was read at 540 nm (with background subtraction at 630 nm) using a BioTek Synergy HT reader and Gen5 2.00 software. Values were normalized to control for each cell line.

Colony formation

Colony formation assays were performed as described previously (30). Briefly, the underlayer was composed of 0.8% SeaPlaque Genetic Technology Grade agarose (50111, Lonza) in DMEM medium containing 10% FBS and antibiotics. Cells were suspended in 0.4% agarose in DMEM medium containing 5% FBS in the overlayer. Medium with or without ASA (1 mmol/L) was replenished twice weekly.

Motility assays

Cell migration and invasion assays were performed as described previously (31). Briefly, cells were pretreated with mitomycin C (10 μg/mL, Sigma) and ASA or PGE_2 (1 μmol/L, Cayman Chemical, #14010, purity >98%) for 2 hours or Compound C (Comp C; dorsomorphin, 0.5 μmol/L, Cayman Chemical, #11967, purity >98%) for 3 hours, then plated onto transwell fibronectin-coated polycarbonate membranes (#3422, Costar) with serum-free medium. Fresh medium containing ASA, 1 μmol/L PGE_2, or 0.5 μmol/L Comp

C was replaced in the lower chamber. For invasion assays, BD BioCoat invasion chambers (354480, Discovery Labware) were used.

Melanin assay

Cells were plated in 6-well dishes plates and incubated with ASA (1 μmol/L), PGE_2 (1 μmol/L), or Comp C (0.5 μmol/L) for 24 hours. After washing with PBS, cells were lysed in each well by the addition of 0.12 mL lysing solution consisting of 1 N sodium hydroxide and 10% DMSO. Lysates were collected and stored at −20 °C. Melanin content was assayed after incubating the lysate at 80°C for 1 hour with occasional vortexing. A synthetic melanin standard (M8631, Sigma) was used to generate a standard curve. Samples were analyzed on a BioTek Synergy HT reader at 470 nm using Gen5 2.00 software. Lysate protein content was determined using a Pierce BCA Protein Assay Kit (Thermo Fisher Scientific) and melanin content was normalized to the protein for each sample.

Mice

NOD/SCID (NOD.CB17-*Prkdc*^{scid}/J) mice purchased from The Jackson Laboratory were maintained in standard conditions. At 7 to 9 weeks of age, animals were given 100 μL of either water or water containing 0.2 to 0.4 mg ASA by oral gavage daily using a sterile stainless steel 20-gauge gavage needle (Cadence Science). ASA was dissolved in sterile distilled water at final concentrations of 1 to 4 mg/mL, and prepared freshly each day. Mice were euthanized by carbon dioxide asphyxiation. Skin was removed using scissors, cut into small pieces, and stored at −80 °C. Blood was obtained by direct cardiac puncture using a sterile 23-gauge hypodermic needle and transferred to EDTA-containing vials (Sarstedt AG & Co.) on ice. Aliquots of whole blood were placed on ice for immunoprofiling (described below). Plasma was obtained by brief centrifugation at 3,000 RPM at 4°C, aliquoted, and immediately frozen at −80 °C. All procedures were conducted under protocol #16–05007, approved by the Institutional Animal Care and Use Committee at the University of Utah (Salt Lake City, UT). Approximately equal numbers of male and female mice were used. We did not observe any differences in response to ASA in male compared with female mice.

Detection of salicylate and PGE_2 by LC/MS

Plasma samples and skin samples were extracted with methyl tert-butyl ether prior to reverse-phase chromatography and analysis by mass spectrometry. Detailed methods are provided in Supplementary Information.

PGE_2 detection by ELISA

PGE_2 content was determined by ELISA using a PGE_2 Assay Kit (KGE004B, R&D Systems) according to the manufacturer's instructions. Frozen tumor samples were homogenized in the supplied buffer, and PGE_2 content was assayed and normalized to protein using the BCA Kit. The ELISA plate was read at 450 nm on a BioTek Synergy spectrophotometer and data were analyzed using Gen5 2.00 software.

Cytokine analysis

Cytokines were simultaneously measured in plasma samples (25 μL) using a ProcartaPlex Multiplex Immunoassay Kit (Invitrogen EPXR360-26092-901) following the manufacturer's instructions. Samples were read on a MAGPI platform Milliplex Map with Luminex xPonent software (MilliporeSigma) for sample acquisition and data were analyzed using accompanying Analyst software.

Tumor production

Mice were shaved on the flank prior to subcutaneous injection of $1–2 \times 10^6$ melanoma cells suspended in 75 μL Matrigel (Corning #354234), which were kept on ice until implanted. Alternatively, while animals were under inhaled isoflurane anesthesia, the implantation site was prepared on shaved skin with alternating betadine and alcohol scrubs. A small incision was made in the skin and 2-mm tumor tissue fragments (that had been stored at −80 °C) were implanted under the skin using sterile technique. For the duration of surgical procedures, mice were kept on a water-circulated heated mat at 37°C. Incisions were then closed with 9-mm wound clips, which remained in place until the wounds had completely healed. Measurements of tumor length, width, and height were recorded twice weekly for tumor volume estimation. Tumors were excised at experimental endpoints and divided into portions stored either at −80 °C or in 10% formalin (Thermo Fisher Scientific) at room temperature.

Analysis of tumor proliferation and apoptosis

Tumors were harvested 2 to 4 hours following ASA gavage. Formalin-fixed tumors were subjected to IHC as described previously (30). Briefly, for assessment of proliferation, sections were stained with a 1:200 dilution of rabbit anti-MIB1 (Ki67, Thermo Fisher Scientific) and a rabbit HRP Kit (Dako K4011), following the manufacturer's instructions. For assessment of apoptosis, TUNEL staining was performed as described previously (32) using an ApopTag Plus Peroxidase In Situ Apoptosis Kit (EMD Millipore), following the manufacturer's instructions.

Western blotting

Western blotting was performed as described previously (31). Briefly, cell pellets were suspended in SDS lysis buffer. Frozen tumor tissues were homogenized in RIPA lysis buffer containing 1.0% NP40, 150 mmol/L NaCl, 50 mmol/L Tris-HCl (pH 8.0), 0.5% sodium deoxycholate, 0.1% SDS, and protease and phosphatase inhibitors. After centrifugation, supernatant was collected and protein estimation was performed by BCA assay. Equal amounts of protein were resolved on 10% SDS polyacrylamide gels, transferred to PVDF membranes, and blocked with 5% nonfat dry milk for 1 hour at room temperature. Thereafter, membranes were probed with primary antibodies against phosphorylated 5′ adenosine monophosphate–activated protein kinase (pAMPK, Cell Signaling Technology 2535, 1:1,000), total AMPK (Santa Cruz Biotechnology sc-74461, 1:2,000), b-actin (Sigma A5316, 1:10,000), tyrosinase (Santa Cruz Biotechnology sc-20035, 1:1,000), MITF (Abcam C5 ab12039, 1:500), phosphorylated ERK (p-ERK, Cell Signaling Technology 9101, 1:1,000), ERK (Cell Signaling Technology 4695, 1:2,000), or tubulin [horseradish

peroxidase (HRP)–tagged, Abcam ab21058, 1:10,000] overnight at 4°C. Membranes were washed, incubated with HRP-conjugated secondary antibody (PerkinElmer, 1:10,000), and then protein bands were visualized using enhanced chemiluminescence (PerkinElmer).

Immunoprofiling of peripheral blood

Whole blood (50 μL) was transferred to flow cytometry tubes and incubated for 30 minutes in the dark at room temperature with 50 μL antibody master mix prepared in PBS containing 0.5% BSA (flow buffer). Red blood cells were then lysed by two rounds of incubation with 2 mL of High-Yield Lyse buffer (Life Technologies) followed by centrifugation at $500 \times g$. Cells were resuspended in flow buffer and analyzed by flow cytometry using either LSRFortessa or FACSCanto instruments (BD Biosciences). Antibodies against CD3ε (Brilliant Violet 421, #100335), CD49b/DX5 (FITC, #108905), and CD11b (APC/Fire 750, #101261) were obtained from BioLegend and used according to the supplier's instructions. Natural killer (NK) cells were identified as the CD3ε-negative, CD49b/DX5– positive population. Neutrophils/monocytes were identified as the CD11b-positive population.

Statistical analysis

Comparisons between experimental groups were analyzed using Student t tests with Prism software (GraphPad), Version 7. For multiple group comparisons, ANOVA was also used. Error bars indicate SEM of triplicate (unless stated otherwise) determinations. P values of 0.05 were considered statistically significant.

Results

ASA inhibits colony formation and motility of melanoma cells and transformed melanocytes

We initially assessed the toxicity of ASA in human melanoma cell lines, transformed human melanocytes, and normal human melanocytes by MTT assay. Although ASA was cytotoxic for normal melanocytes at concentrations >1 mmol/L, the viability of melanoma cells and transformed melanocytes was not affected by ASA over 24 to 48 hours at concentrations below 1.5 mmol/L (Supplementary Fig. S1). The ability to form colonies in soft agar is a surrogate for tumor growth. We assessed the capacity of ASA to block colony formation, which was significantly reduced in ASA-treated A375 and MTG2 cells (Fig. 1A) and Mel-STR cells (Fig. 1B). In transwell assays, 1 mmol/L ASA significantly inhibited the migration of A375, YU2, WM3311 (not shown), and MTG2 cells (Fig. 2A), as well as Mel-STM and Mel-STR cells (Fig. 2B). Similarly, in Matrigel invasion assays, melanoma cells (Fig. 2C) and transformed melanocytes (Fig. 2D) were significantly inhibited by ASA. In addition, we observed that the COX-2–specific inhibitor, celecoxib, significantly inhibited migration of A375 and Mel-STM cells at concentrations of 20 or 40 μmol/L (Supplementary Fig. S2A), which did not affect cell viability in MTT assays (Supplementary Fig. S2B). Thus, it is likely that ASA blocks cell migration through inhibition of COX-2.

Rescue of ASA-mediated inhibition of migration by Comp C and PGE$_2$

Several reports have demonstrated activation of AMPK by ASA (9) and suggested that AMPK activation contributes to the antitumor effects of ASA (10, 11). Consistent with these

prior reports, we found that ASA activated AMPK in A375, MTG2, and Mel-STM cells, as reflected by 3- to 5-fold increase in the phosphorylated species (Fig. 3A). Treatment with the AMPK inhibitor Comp C reduced levels of phosphorylated AMPK to that of control cells (Fig. 3A). We confirmed that ASA suppressed synthesis of PGE_2 in these cells (Fig. 3B). Although addition of Comp C alone also suppressed PGE_2 production (but to a lesser extent than ASA), its addition partially restored PGE_2 levels in ASA-treated cells (Fig. 3B), suggesting that AMPK activation is at least partially responsible for ASA-mediated suppression of PGE_2. In migration assays, addition of Comp C restored the migratory capacity of ASA-treated A375 (Fig. 3C), Mel-STM (Fig. 3D), and MTG2 cells (Fig. 3E) to that of untreated cells. Similarly, addition of PGE_2 also restored the migratory capacity of ASA-treated A375 (Fig. 3C), Mel-STM (Fig. 3D), and MTG2 cells (Fig. 3E). Thus, inhibition of migration by ASA appears to be mediated by activated AMPK and suppression of PGE_2, as inhibition of AMPK activation or addition of PGE_2 was able to rescue ASA-treated cells in the migration assay.

ASA inhibits melanin synthesis

The ability to synthesize melanin is a unique property of melanocytic cells. Both ASA and celecoxib treatment reduced pigmentation in B16 and MTG2 cells, which could be appreciated by visual examination of cell pellets (Fig. 4A). Melanin production, quantitated spectroscopically, was significantly reduced in ASA or celecoxib-treated B16, MTG2, and WM3311 cells (Fig. 4B). We next examined whether ASA-mediated inhibition of melanin production could be rescued by either addition of Comp C or PGE_2. Although Comp C and PGE_2 caused some reduction in melanin production in B16 cells, the addition of either resulted in significantly higher levels of melanin in ASA-treated cells (Fig. 4C). Similarly, both Comp C and PGE_2 were independently able to rescue ASA-mediated inhibition of melanin production in MTG2 cells (Fig. 4D). Despite the significant effects on melanin production, ASA treatment did not markedly affect levels of tyrosinase, MITF, or p-ERK in either MTG2 or WM3311 cells (Fig. 4E).

Chronic orally delivered ASA is well tolerated

Next, we developed an animal model to investigate the antitumor effects of ASA *in vivo*. In a pilot experiment, we assessed the tolerability of daily ASA gavage over a period of one month by monitoring body weight. As shown in Supplementary Fig. S3, chronic daily gavage with 100 μL water or 100 μL water containing 0.2 to 0.4 mg ASA was well tolerated in NOD/SCID mice, which we planned to use as hosts for PDX lines as described below.

Salicylate and PGE_2 in blood and skin following ASA dosing

To assess the metabolism of ASA following oral dosing, blood and skin samples were collected from animals prior to ASA treatment (controls, 0 hour) and at time points between 4 and 24 hours following a single dose of 0.4 mg ASA by gavage. ASA is known to be rapidly metabolized after digestion (33). We detected significant elevation of the immediate metabolite of ASA, salicylic acid (salicylate), in plasma at 4 hours posttreatment; plasma salicylate levels had significantly diminished by 8 hours and returned to background by 12 hours (Fig. 5A, left). Plasma PGE_2 was detectable prior to ASA exposure, significantly decreased by 8 hours and remained undetectable at 24 hours following ASA dosing (Fig.

5A, right). Similar trends were observed in mouse skin (Fig. 5B). Thus, salicylate can be detected in skin following oral delivery and is associated with rapid and prolonged suppression of PGE_2 levels in blood and skin.

Sensitivity of human melanoma xenografts to ASA

MTG2 cells exhibited robust tumor formation in NOD/SCID (control) mice, while their tumor development was significantly delayed in animals treated with ASA beginning one week prior to and following cell implantation (Fig. 6A, left; Supplementary Fig. S4). Tumor development was also significantly delayed, although to a lesser degree, in ASA-treated animals implanted with MTG2 tumor fragments (Fig. 6A, right). MTG4 cells also exhibited significantly delayed tumor development in ASA-treated compared with control animals (Fig. 6B, left), although a significant difference in tumor growth was not seen in animals implanted with MTG4 tumor fragments (Fig. 6B, right). In contrast, both A375 and WM3311 melanoma cell lines were resistant to ASA, as tumor development was not significantly different in control versus ASA-treated animals (Fig. 6C). Similarly, tumor development by MTG5 cells or tumor fragments and Mel-STR cells was not significantly impacted by ASA treatment (Supplementary Fig. S5). Thus, some tumors were sensitive to ASA, whereas others were resistant, and for ASA-sensitive tumors, the inhibitory effect of ASA on tumor development was more pronounced when cells compared with tumor fragments were implanted.

ASA inhibits proliferation of sensitive tumors

To gain insight into the differential effects of ASA on tumor growth, we examined markers of proliferation and apoptosis in cell-implanted tumors that were sensitive (MTG2), partially sensitive (MTG4), and resistant (A375) to ASA. Staining for the mitotic marker Ki67 (MIB-1) revealed significantly lower rates of proliferation in ASA-exposed compared with control MTG2 and MTG4 tumors, while ASA did not significantly impact proliferation of A375 tumors (Fig. 7A). However, staining for TUNEL-positive cells did not demonstrate significant differences in tumor cell apoptosis between control and ASA-exposed tumors for any of the three tumor types (Fig. 7B). Thus, sensitivity to ASA correlated with reduced proliferation rather than increased apoptosis in tumors from animals chronically treated with ASA.

ASA suppresses PGE_2 and activates AMPK in both sensitive and resistant tumors

We next examined PGE_2 levels and signaling in cell-implanted tumors that were sensitive (MTG2) and resistant (A375) to ASA. As shown in Fig. 7C, PGE_2 levels were significantly reduced (by ~50%) in both MTG2 and A375 tumors, although PGE_2 levels were much higher in ASA-resistant A375 than ASA-sensitive MTG2 tumors. Next, we assessed AMPK activation in control and ASA-exposed tumors. We observed increased phosphorylated AMPK associated with ASA exposure in both ASA-sensitive MTG2 and ASA-resistant A375 tumors (Fig. 7D). Thus, suppression of PGE_2 and activation of AMPK are unlikely to explain fully the differential sensitivity of tumors to ASA, although high residual PGE_2 levels in ASA-treated A375 tumors may have contributed to ASA resistance.

ASA inhibits growth of established tumors

Tumor fragments may be more similar to an established tumor than a cell line. Given the difference in tumor sensitivity of ASA between implants of cells versus fragments for MTG2 and MTG4, we examined whether ASA could affect growth of established tumors. We initiated treatment with water (control) or ASA in groups of mice one week prior to implantation with MTG2 cells as described above. A third group of mice (ASA-delay) was implanted with MTG2 cells, but daily ASA gavage was initiated when tumors reached 5 mm in diameter. As shown in Fig. 8A, both the ASA-treated and ASA-delay groups demonstrated similar patterns of tumor growth, which were significantly reduced compared with the control group. Levels of PGE_2 in plasma and tumors (obtained at experimental endpoint) were comparable between the ASA-treated and ASA-delay groups and were significantly lower than that of the control group (Fig. 8B). Thus, ASA was able to reduce MTG2 tumor growth whether initiated prior to tumor cell inoculation or once small tumors were established.

Immunoprofiling of mice following chronic ASA exposure

NOD/SCID mice lack functional T- and B lymphocytes associated with acquired immunologic memory, but retain an innate immune system constituted by NK cells and neutrophil/mononuclear cells (34). To assess the impact of chronic ASA exposure on the peripheral immune system, we performed immuneprofiling of peripheral blood taken from both control and ASA-treated animals (at experimental endpoint) in the MTG2 ASA-delay experiment described above. The NK cell ($DX5^+CD3^-$) and neutrophil/monocyte ($CD11b^+GR1^-$) compartments were not significantly different between the control and ASA-treated animals (Fig. 8C). Similarly, we did not observe differences in immune cell compartments in control and ASA-treated animals bearing WM3311 tumors (not shown). Finally, we analyzed plasma cytokine profiles from these animals. As shown in Fig. 8D, levels of $IFN\gamma$ and IL3 were reduced, whereas IL5 and IL28 were elevated in ASA-treated compared with control animals. Significant differences were not observed for IL4, IL6, IL17a, IL18, IL22, IL31, LIF, IP-10, GRO-α, MCP-1, MCP-3, MIP-2, Eotaxin, or ENA-78. The quantitative data for the entire panel of cytokines tested are shown in Supplementary Fig. S6. The following cytokines were not detected: $IL1\alpha$, $IL1\beta$, IL2, IL9, IL10, $IL12\beta$, IL13, IL15, IL23, IL27, RANTES, $TNF\alpha$, $IFN\alpha$, MIP-1, G-CSF, M-CSF, and GM-CSF (not shown).

Discussion

The chemopreventive and anticarcinogenic activities of ASA have largely been attributed to COX inhibition resulting in reduced synthesis of PGE_2, which is upregulated in cancers (3) and implicated in multiple carcinogenic processes (5–8). In addition, ASA has been shown to activate the ATM kinase (35) and block NFκB (36) and Akt pathways (37). Other activities of ASA include activation of AMPK (9) that may regulate mTOR pathways involved in autophagy (11) and apoptosis (10) in cancer cells, and inhibition of heparanase that was associated with reduced angiogenesis and growth of tumor xenografts (22). In some cases, these "COX-independent" activities were observed at much higher concentrations (i.e., 5 mmol/L) than required for COX inhibition and thus may not be clinically relevant (38). Although other cancer cell types (e.g., colon, breast) demonstrated cytotoxicity to ASA

at concentrations below 1 mmol/L (39), we found that ASA at a concentration of 1 mmol/L was not cytotoxic for our panel of melanoma lines. This concentration seems physiologically relevant, as plasma concentrations of ASA were not found to exceed 2 mmol/L in patients treated for rheumatoid arthritis (40). Here, we report that 1 mmol/L ASA was able to significantly inhibit melanoma cell motility and melanin synthesis, which could be reversed by addition of PGE_2 or recapitulated by the COX-2–selective inhibitor celecoxib, suggesting that inhibition of COX-2/PGE_2 is sufficient for these effects observed with ASA.

The ability of the AMPK inhibitor Comp C to restore (at least partially) PGE_2 levels in ASA-treated cells and rescue ASA-mediated inhibition of migration and melanin synthesis suggests that the COX-2 and AMPK pathways may be interrelated. Indeed, multiple studies have suggested that AMPK is downstream of PGE_2, although there are conflicting reports as to whether AMPK is positively or negatively regulated by PGE_2. Funahashi and colleagues (41) observed that PGE_2 negatively regulates AMPK phosphorylation, whereas others showed that PGE_2 stimulated AMPK phosphorylation (42, 43). In addition, several studies have demonstrated a positive feedback loop in which AMPK upregulates COX-2 (44, 45). This regulatory circuit involving AMPK-mediated upregulation of COX-2 may be operative in melanoma cells, as we observed that Comp C caused a small but significant reduction in PGE_2 levels; however, this effect was overridden in ASA-treated cells in which the addition of Comp C partially restored PGE_2 levels, migratory capacity, and melanin synthesis. Although Nishio and colleagues (46) reported that melanin production was inhibited by ASA in B16-F10 cells at concentrations of 2 to 3 mmol/L and associated with downregulation of MITF and pERK, we found that 1 mmol/L ASA significantly blocked melanin synthesis without affecting MITF or pERK levels and could be rescued by either exogenous PGE_2 or inhibition of AMPK.

Previous preclinical studies examining the effects of ASA on melanoma *in vivo* have been problematic, either because extremely high nonphysiologic doses (up to 250 mg/kg) were delivered intraperitoneally (20, 22) or ASA was dissolved in the drinking water (21), where the amount of active drug delivered was sporadic and could not be controlled. In the current study, we avoided these pitfalls by delivering ASA by oral gavage, which was well tolerated and resulted in detectable levels of salicylate in both the blood and skin. At 4 hours following an oral dose of 0.4 mg ASA, we detected salicylate levels of approximately 4,000 to 7,000 ng/mL above background in plasma. In comparison, using the same LC/MS methods, we have detected plasma salicylate levels in the range of 200 to 1,000 ng/mL in human subjects following oral ingestion of a single 325 mg ASA tablet (Rahman and Grossman, unpublished). Thus, the mouse model described here appears to be suitable for preclinical ASA chemoprevention studies in anticipation of human chemoprevention trials involving daily oral ASA dosing. Although higher oral ASA dosing could potentially be achieved, the salicylate concentrations we detected in plasma were physiologic and sufficient to suppress PGE_2 levels in blood, skin, and xenografted tumors.

It is unclear why some tumors were sensitive, whereas others were resistant to ASA. Although ASA significantly reduced PGE_2 levels in both sensitive (MTG2) and resistant (A375) tumors, PGE_2 levels were much higher in control and ASA-treated A375 versus MTG2 tumors. Thus, it is possible that residual levels of PGE_2 in ASA-treated A375 tumors

were sufficient to sustain tumor growth. Alternatively, it is conceivable that in some tumors redundant signaling molecules or pathways independent of PGE_2 are required for tumor development and growth so that reduction in PGE_2 levels is inconsequential. Activation of AMPK signaling has been associated with antitumor effects of ASA (10, 11); however, we observed increased levels of phosphorylated AMPK in both ASA-sensitive and resistant tumors. Henry and colleagues (47) reported that ASA decreased viability and anchorage-independent growth of mutant PIK3CA (but not wild-type PIK3CA) breast cancer cells independently of its effects on COX-2; however, we have not characterized our panel of melanoma lines for PIK3CA mutations or expression.

Tumors in which growth was reduced by ASA treatment demonstrated decreased proliferation rather than increased apoptosis. For these ASA-sensitive tumors, the inhibition of tumor growth was more pronounced for cell implants compared with tumor fragments. This difference may reflect the importance of established tumor microenvironment and its constituent intercellular interactions. On the other hand, we found that for one tumor line (MTG2), tumor growth was inhibited as efficiently when ASA treatment was initiated after tumors were established. This result suggests that prolonged pretreatment with ASA may not be necessary for its chemoprotective effects.

Finally, the immunodeficient mouse host that was employed to accommodate human tumor xenografts did not exhibit marked inflammation in the skin or tumor, and there was minimal alteration in the percentage of NK cells and neutrophils or pattern of cytokine expression in the blood of ASA-treated animals. We plan to extend these studies into immunocompetent mouse strains with genetic susceptibility to UV-induced melanoma (48, 49). Such tumor models may be more amenable to ASA-mediated prevention or inhibition of tumor growth given the inflammation and increased PGE_2 associated with UV-irradiation of the skin (50). In addition, such models would allow us to test the capacity of ASA to block development of de novo melanoma, which may be more directly relevant to chemoprevention.

In summary, we have shown that ASA inhibits melanoma cell motility, colony formation, and pigmentation through suppression of PGE_2 and activation of AMPK, and that daily oral ASA suppresses PGE_2 in mouse blood, skin, and tumors, although these activities were not sufficient to inhibit growth of some melanoma tumors *in vivo*. This model could be used for investigating other biomarkers relevant to ASA metabolism and tumor development and metastasis, and responses of melanoma tumors driven by different oncogenic mutations. Such preclinical data will be important to support future melanoma chemoprevention trials in humans.

Supplementary Material

Refer to Web version on PubMed Central for supplementary material.

Acknowledgments

References

1. Desborough MJ, Keeling DM. The aspirin story - from willow to wonder drug. Br J Haematol 2017;177:674–83. [PubMed: 28106908]

2. Van Der Ouderaa FJ, Buytenhek M, Nugteren DH, Van Dorp DA. Acetylation of prostaglandin endoperoxide synthetase with acetylsalicylic acid. Eur J Biochem 1980;109:1–8. [PubMed: 6773769]

3. Block KI. Inflammation, COX-2 inhibitors, and cancer. Integr Cancer Ther 2005;4:3–4. [PubMed: 15695470]

4. Solomon SD, McMurray JJ, Pfeffer MA, Wittes J, Fowler R, Finn P, et al. Cardiovascular risk associated with celecoxib in a clinical trial for colorectal adenoma prevention. N Engl J Med 2005; 352:1071–80. [PubMed: 15713944]

5. Jain S, Chakraborty G, Raja R, Kale S, Kundu GC. Prostaglandin E2 regulates tumor angiogenesis in prostate cancer. Cancer Res 2008; 68:7750–9. [PubMed: 18829529]

6. Abrahao AC, Castilho RM, Squarize CH, Molinolo AA, dos Santos-Pinto D Jr, Gutkind JS. A role for COX2-derived PGE2 and PGE2-receptor subtypes in head and neck squamous carcinoma cell proliferation. Oral Oncol 2010;46:880–7. [PubMed: 20951077]

7. Mayoral R, Fernandez-Martinez A, Bosca L, Martin-Sanz P. Prostaglandin E2 promotes migration and adhesion in hepatocellular carcinoma cells. Carcinogenesis 2005;26:753–61. [PubMed: 15661807]

8. Li Z, Zhang Y, Kim WJ, Daaka Y. PGE2 promotes renal carcinoma cell invasion through activated RalA. Oncogene 2013;32: 1408–15. [PubMed: 22580611]

9. Hawley SA, Fullerton MD, Ross FA, Schertzer JD, Chevtzoff C, Walker KJ, et al. The ancient drug salicylate directly activates AMP-activated protein kinase. Science 2012;336:918–22. [PubMed: 22517326]

10. Gao M, Kong Q, Hua H, Yin Y, Wang J, Luo T, et al. AMPK-mediated up-regulation of mTORC2 and MCL-1 compromises the anti-cancer effects of aspirin. Oncotarget 2016;7:16349–61. [PubMed: 26918349]

11. Din FV, Valanciute A, Houde VP, Zibrova D, Green KA, Sakamoto K, et al. Aspirin inhibits mTOR signaling, activates AMP-activated protein kinase, and induces autophagy in colorectal cancer cells. Gastroenterology 2012;142:1504–15 e3. [PubMed: 22406476]

12. Chan AT, Arber N, Burn J, Chia WK, Elwood P, Hull MA, et al. Aspirin in the chemoprevention of colorectal neoplasia: an overview. Cancer Prev Res (Phila) 2012;5:164–78. [PubMed: 22084361]

13. Ye X, Fu J, Yang Y, Gao Y, Liu L, Chen S. Frequency-risk and duration-risk relationships between aspirin use and gastric cancer: a systematic review and meta-analysis. PLoS One 2013;8: e71522. [PubMed: 23936269]

14. Swede H, Mirand AL, Menezes RJ, Moysich KB. Association of regular aspirin use and breast cancer risk. Oncology 2005; 68:40–7. [PubMed: 15802928]

15. Salinas CA, Kwon EM, FitzGerald LM, Feng Z, Nelson PS, Ostrander EA, et al. Use of aspirin and other nonsteroidal antiinflammatory medications in relation to prostate cancer risk. Am J Epidemiol 2010;172:578–90. [PubMed: 20688905]

16. Goodman JR, Grossman D. Aspirin and other NSAIDs as chemoprevention agents in melanoma. Cancer Prev Res 2014; 7:557–64.

17. Sorensen HT, Friis S, Norgard B, Mellemkjaer L, Blot WJ, McLaughlin JK, et al. Risk of cancer in a large cohort of nonaspirin NSAID users: a population-based study. Br J Cancer 2003;88: 1687–92. [PubMed: 12771981]

18. Jacobs EJ, Thun MJ, Bain EB, Rodriguez C, Henley SJ, Calle EE. A large cohort study of long-term daily use of adult-strength aspirin and cancer incidence. J Natl Cancer Inst 2007;99:608–15. [PubMed: 17440162]

19. Gamba CA, Swetter SM, Stefanick ML, Kubo J, Desai M, Spaunhurst KM, et al. Aspirin is associated with lower melanoma risk among postmenopausal Caucasian women: the Women's Health Initiative. Cancer 2013;119:1562–9. [PubMed: 23483536]

20. Vad NM, Kudugunti SK, Wang H, Bhat GJ, Moridani MY. Efficacy of acetylsalicylic acid (aspirin) in skin B16-F0 melanoma tumor-bearing C57BL/6 mice. Tumour Biol 2014;35: 4967–76. [PubMed: 24492939]

21. Zelenay S, van der Veen AG, Bottcher JP, Snelgrove KJ, Rogers N, Acton SE, et al. Cyclooxygenase-dependent tumor growth through evasion of immunity. Cell 2015;162:1257–70. [PubMed: 26343581]

22. Dai X, Yan J, Fu X, Pan Q, Sun D, Xu Y, et al. Aspirin inhibits cancer metastasis and angiogenesis via targeting heparanase. Clin Cancer Res 2017;23:6267–78. [PubMed: 28710312]

23. Kuzbicki L, Lange D, Straczynska-Niemiec A, Chwirot BW. The value of cyclooxygenase-2 expression in differentiating between early melanomas and histopathologically difficult types of benign human skin lesions. Melanoma Res 2012;22:70–6. [PubMed: 22228276]

24. Kuzbicki L, Sarnecka A, Chwirot BW. Expression of cyclooxygenase-2 in benign naevi and during human cutaneous melanoma progression. Melanoma Res 2006;16:29–36. [PubMed: 16432453]

25. Becker MR, Siegelin MD, Rompel R, Enk AH, Gaiser T. COX-2 expression in malignant melanoma: a novel prognostic marker? Melanoma Res 2009;19:8–16. [PubMed: 19430402]

26. Fang D, Nguyen TK, Leishear K, Finko R, Kulp AN, Hotz S, et al. A tumorigenic subpopulation with stem cell properties in melanomas. Cancer Res 2005;65:9328–37. [PubMed: 16230395]

27. Grossman D, McNiff JM, Li F, Altieri DC. Expression and targeting of the apoptosis inhibitor, survivin, in human melanoma. J Invest Dermatol 1999;113:1076–81. [PubMed: 10594755]

28. Bowen AR, Hanks AN, Allen SM, Alexander A, Diedrich MJ, Grossman D. Apoptosis regulators and responses in human melanocytic and keratinocytic cells. J Invest Dermatol 2003; 120:48–55. [PubMed: 12535197]

29. Gupta PB, Kuperwasser C, Brunet JP, Ramaswamy S, Kuo WL, Gray JW, et al. The melanocyte differentiation program predisposes to metastasis after neoplastic transformation. Nat Genet 2005;37:1047–54. [PubMed: 16142232]

30. McKenzie JA, Liu T, Jung JY, Jones BB, Ekiz HA, Welm AL, et al. Survivin promotion of melanoma metastasis requires upregulation of alpha5 integrin. Carcinogenesis 2013;34:2137–44. [PubMed: 23640047]

31. McKenzie JA, Liu T, Goodson AG, Grossman D. Survivin enhances motility of melanoma cells by supporting Akt activation and {alpha}5 integrin upregulation. Cancer Res 2010; 70:7927–37. [PubMed: 20807805]

32. Thomas J, Liu T, Cotter MA, Florell SR, Robinette K, Hanks AN, et al. Melanocyte expression of survivin promotes development and metastasis of UV-induced melanoma in HGF-transgenic mice. Cancer Res 2007;67:5172–8. [PubMed: 17545596]

33. Needs CJ, Brooks PM. Clinical pharmacokinetics of the salicylates. Clin Pharmacokinet 1985;10:164–77. [PubMed: 3888490]

34. Hudson WA, Li Q, Le C, Kersey JH. Xenotransplantation of human lymphoid malignancies is optimized in mice with multiple immunologic defects. Leukemia 1998;12:2029–33. [PubMed: 9844934]

35. Luciani MG, Campregher C, Gasche C. Aspirin blocks proliferation in colon cells by inducing a G1 arrest and apoptosis through activation of the checkpoint kinase ATM. Carcinogenesis 2007;28:2207–17. [PubMed: 17510082]

36. Liao D, Zhong L, Duan T, Zhang RH, Wang X, Wang G, et al. Aspirin suppresses the growth and metastasis of osteosarcoma through the NF-kappaB pathway. Clin Cancer Res 2015;21: 5349–59. [PubMed: 26202947]

37. Fernandez HR, Linden SK. The aspirin metabolite salicylate inhibits lysine acetyltransferases and MUC1 induced epithelial to mesenchymal transition. Sci Rep 2017;7:5626. [PubMed: 28717171]

38. Steinberg GR, Dandapani M, Hardie DG. AMPK: mediating the metabolic effects of salicylate-based drugs? Trends Endocrinol Metab 2013;24:481–7. [PubMed: 23871515]

39. Dachineni R, Ai G, Kumar DR, Sadhu SS, Tummala H, Bhat GJ. Cyclin A2 and CDK2 as novel targets of aspirin and salicylic acid: a potential role in cancer prevention. Mol Cancer Res 2016;14: 241–52. [PubMed: 26685215]

40. Preston SJ, Arnold MH, Beller EM, Brooks PM, Buchanan WW. Comparative analgesic and anti-inflammatory properties of sodium salicylate and acetylsalicylic acid (aspirin) in rheumatoid arthritis. Br J Clin Pharmacol 1989;27:607–11. [PubMed: 2788004]

41. Funahashi K, Cao X, Yamauchi M, Kozaki Y, Ishiguro N, Kambe F. Prostaglandin E2 negatively regulates AMP-activated protein kinase via protein kinase A signaling pathway. Prostaglandins Other Lipid Mediat 2009;88:31–5. [PubMed: 18832041]

42. Kainuma S, Otsuka T, Kuroyanagi G, Yamamoto N, Matsushima-Nishiwaki R, Kozawa O, et al. Regulation by AMP-activated protein kinase of PGE2-induced osteoprotegerin synthesis in osteoblasts. Mol Med Rep 2016;13:3363–9. [PubMed: 26935864]

43. Zhu Z, Fu C, Li X, Song Y, Li C, Zou M, et al. Prostaglandin E2 promotes endothelial differentiation from bone marrow-derived cells through AMPK activation. PLoS One 2011;6: e23554. [PubMed: 21876756]

44. Zhang J, Bowden GT. UVB irradiation regulates Cox-2 mRNA stability through AMPK and HuR in human keratinocytes. Mol Carcinog 2008;47:974–83. [PubMed: 18449856]

45. Lee S, Jeong S, Kim W, Kim D, Yang Y, Yoon JH, et al. Rebamipide induces the gastric mucosal protective factor, cyclooxygenase-2, via activation of 5'-AMP-activated protein kinase. Biochem Biophys Res Commun 2017;483:449–55. [PubMed: 28011266]

46. Nishio T, Usami M, Awaji M, Shinohara S, Sato K. Dual effects of acetylsalicylic acid on ERK signaling and Mitf transcription lead to inhibition of melanogenesis. Mol Cell Biochem 2016;412: 101–10. [PubMed: 26699907]

47. Henry WS, Laszewski T, Tsang T, Beca F, Beck AH, McAllister SS, et al. Aspirin suppresses growth in PI3K-mutant breast cancer by activating AMPK and inhibiting mTORC1 signaling. Cancer Res 2017;77:790–801. [PubMed: 27940576]

48. Viros A, Sanchez-Laorden B, Pedersen M, Furney SJ, Rae J, Hogan K, et al. Ultraviolet radiation accelerates BRAF-driven melanomagenesis by targeting TP53. Nature 2014;511: 478–82. [PubMed: 24919155]

49. Hennessey RC, Holderbaum AM, Bonilla A, Delaney C, Gillahan JE, Tober KL, et al. Ultraviolet radiation accelerates NRas-mutant melanomagenesis: a cooperative effect blocked by sunscreen. Pigment Cell Melanoma Res 2017;30:477–87. [PubMed: 28544727]

50. Gledhill K, Rhodes LE, Brownrigg M, Haylett AK, Masoodi M, Thody AJ, et al. Prostaglandin-E2 is produced by adult human epidermal melanocytes in response to UVB in a melanogenesis-independent manner. Pigment Cell Melanoma Res 2010;23: 394–403. [PubMed: 20236442]
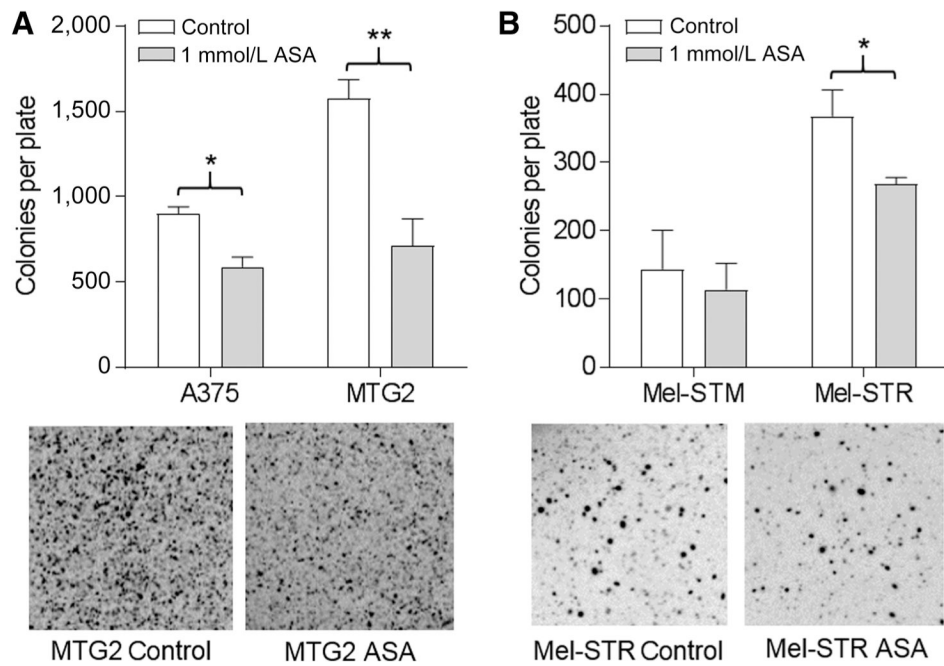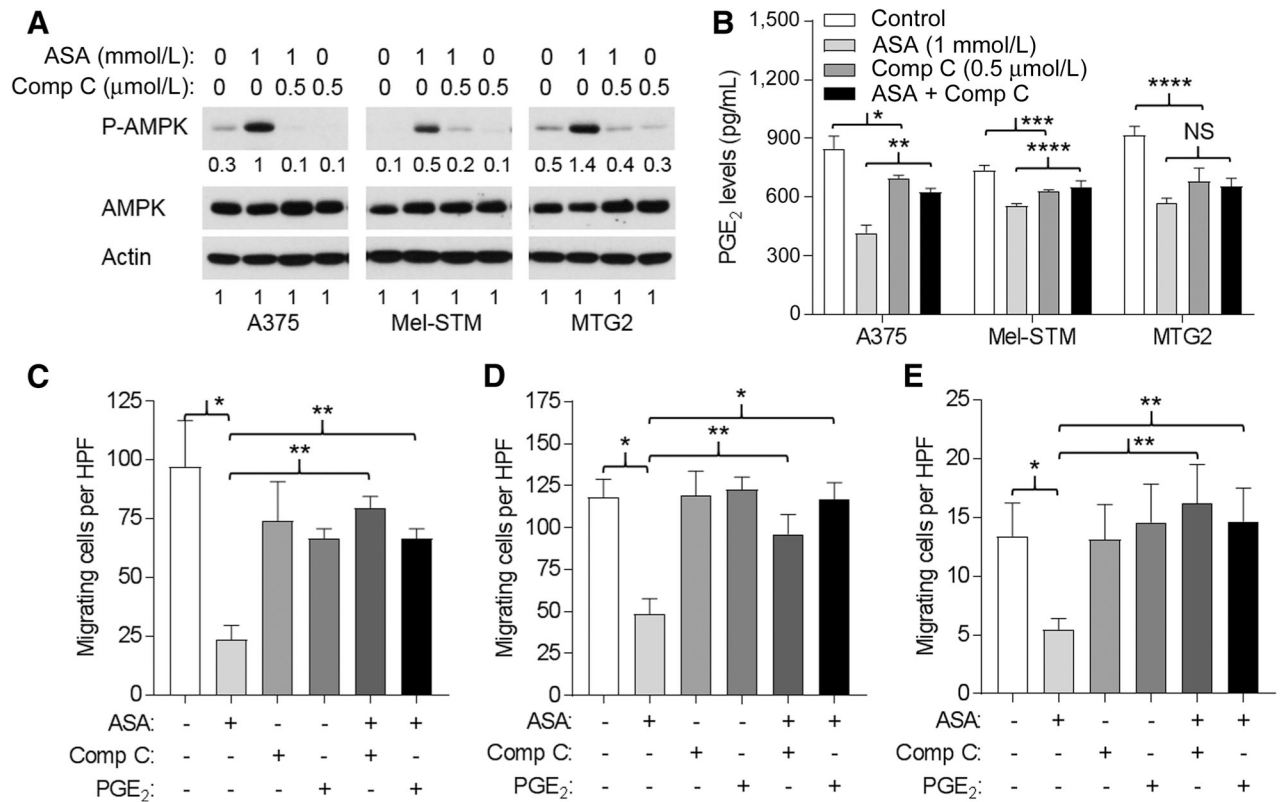
Figure 1.
Colony formation is inhibited by ASA. **A,** Cells were grown in agarose in the absence (control) or presence of ASA; then, colonies were counted. *, $P = 0.03$; **, $P = 0.01$. Photos shown are of representative MTG2 plates. **B,** Colony formation of melanocyte lines as in **A.** *, $P = 0.06$. Photos shown are of representative Mel-STR plates.
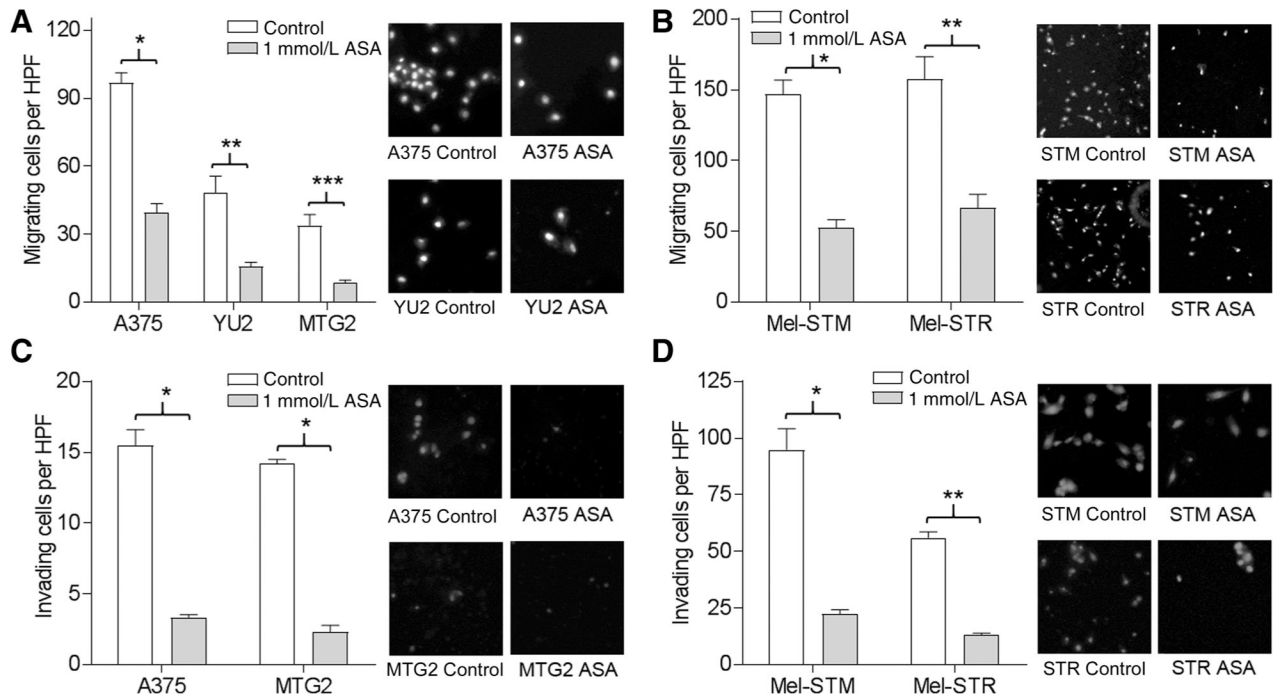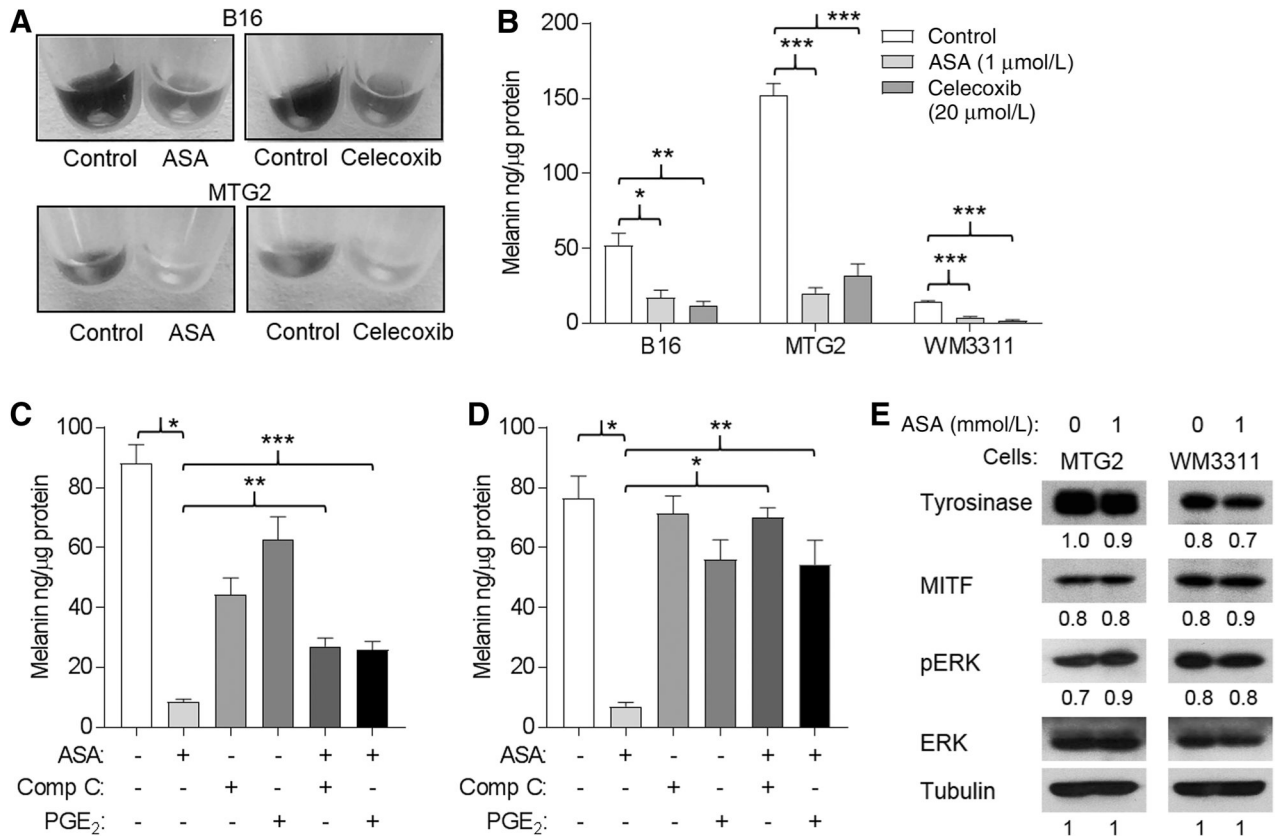
Figure 2.
ASA impairs cell motility. **A,** Melanoma lines were subjected to migration assay in the absence (control) or presence of ASA for 24 hours. *, $P < 0.001$; **, $P = 0.01$; ***, $P = 0.007$. Photos shown are of representative high-power field (HPF, ×200). **B,** Melanocyte lines were treated as in **A.** *, $P = 0.001$; **, $P = 0.01$. **C,** Melanoma lines treated as in **A** were subjected to invasion assay with or without (control) ASA for 48 hours. *, $P < 0.001$. **D,** Melanocyte lines were treated as in **C.** *, $P < 0.002$; **, $P < 0.001$.
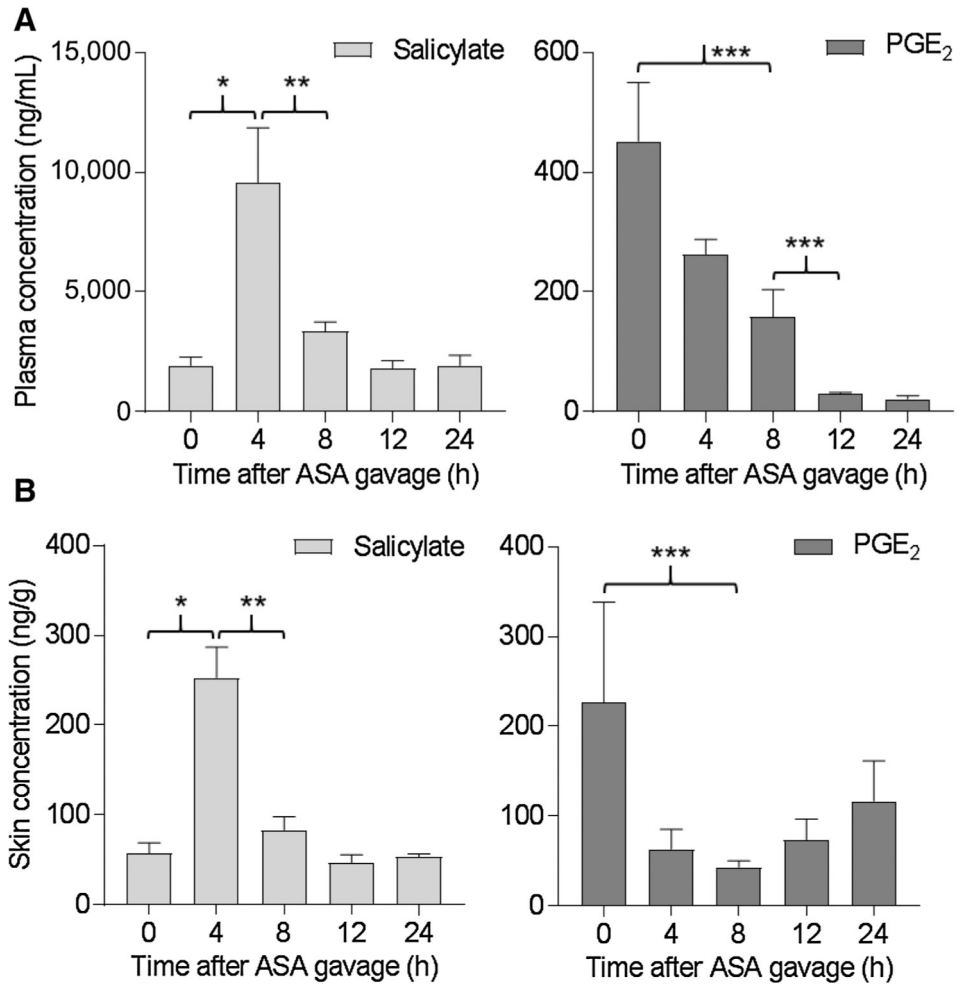
Figure 3.
ASA-mediated inhibition of migration reversed by Comp C and PGE_2. **A,** Western blots of cells after treatment with ASA and/or Comp C for 24 hours. Representative blot from two experiments. Numbers are from densitometry scan. **B,** PGE_2 concentrations of supernatants from cells incubated 24 hours with ASA, Comp C, or both (Comp C added 1 hour before ASA) as indicated. For ANOVA, $P < 0.001$ for each cell type. For *t* test comparisons: *, $P = 0.08$; **, $P = 0.009$; ***, $P = 0.02$; ***, $P = 0.05$. NS, not significant. **C,** Migration (24 hours) of A375 cells per high-power field (HPF) in the absence or presence 1 mmol/L ASA, 0.5 μmol/L Comp C, and 1 μmol/L PGE_2 as indicated. Comp C or PGE_2 was added 1 hour before ASA. For ANOVA, $P < 0.001$. For *t* test comparisons: *, $P = 0.004$; **, $P < 0.001$. **D,** Migration of Mel-STM cells as in **C.** For ANOVA, $P = 0.003$. For *t* test comparisons: *, $P = 0.008$; **, $P = 0.03$. **E,** Migration of MTG2 cells as in **C.** For ANOVA, $P = 0.005$. For *t* test comparisons: *, $P = 0.05$; **, $P = 0.04$.
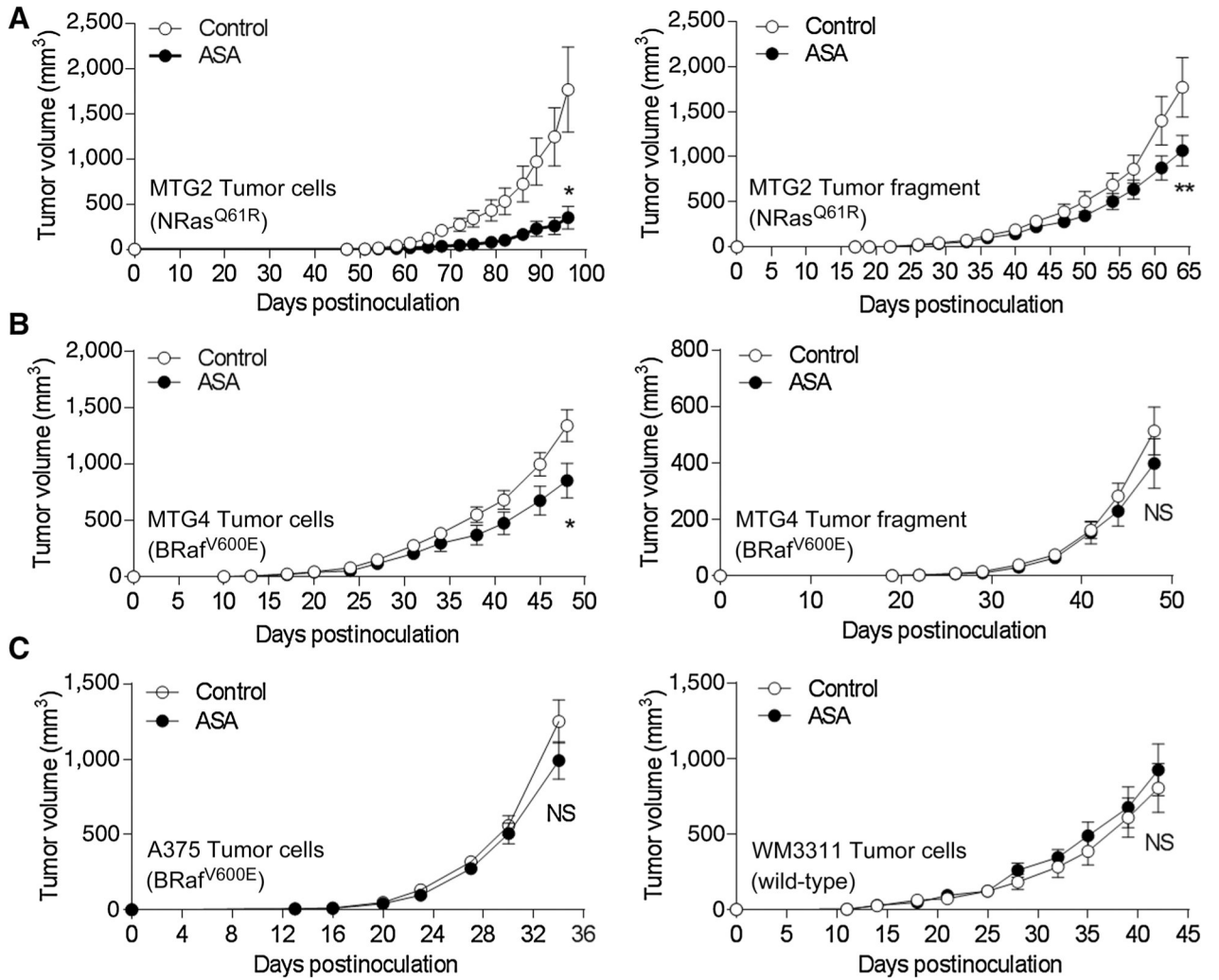
Figure 4.
Melanin production is inhibited by ASA and rescued by PGE$_2$. **A,** Melanoma cells were incubated in the absence (control) or presence of ASA or celecoxib for 24 hours; then, melanin was quantitated in cell lysates. *, $P = 0.02$; **, $P = 0.01$; ***, $P < 0.001$. **B,** Representative photos shown of cell pellets. **C,** B16 cells were incubated for 24 hours in the absence or presence of 1 mmol/L ASA, 0.5 μmol/L Comp C, and/or 1 μmol/L PGE$_2$ as indicated. Comp C or PGE$_2$ was added 1 hour before ASA. For ANOVA, $P < 0.001$. For t test comparisons: *, $P < 0.001$; **, $P = 0.003$; ***, $P = 0.005$. **D,** MTG2 cells were treated as in C. For ANOVA, $P < 0.001$. For t test comparisons: *, $P < 0.001$; **, $P = 0.005$. **E,** Western blots for tyrosinase, MITF, and p-ERK. Representative blot is from two experiments. Numbers are from densitometry scan.
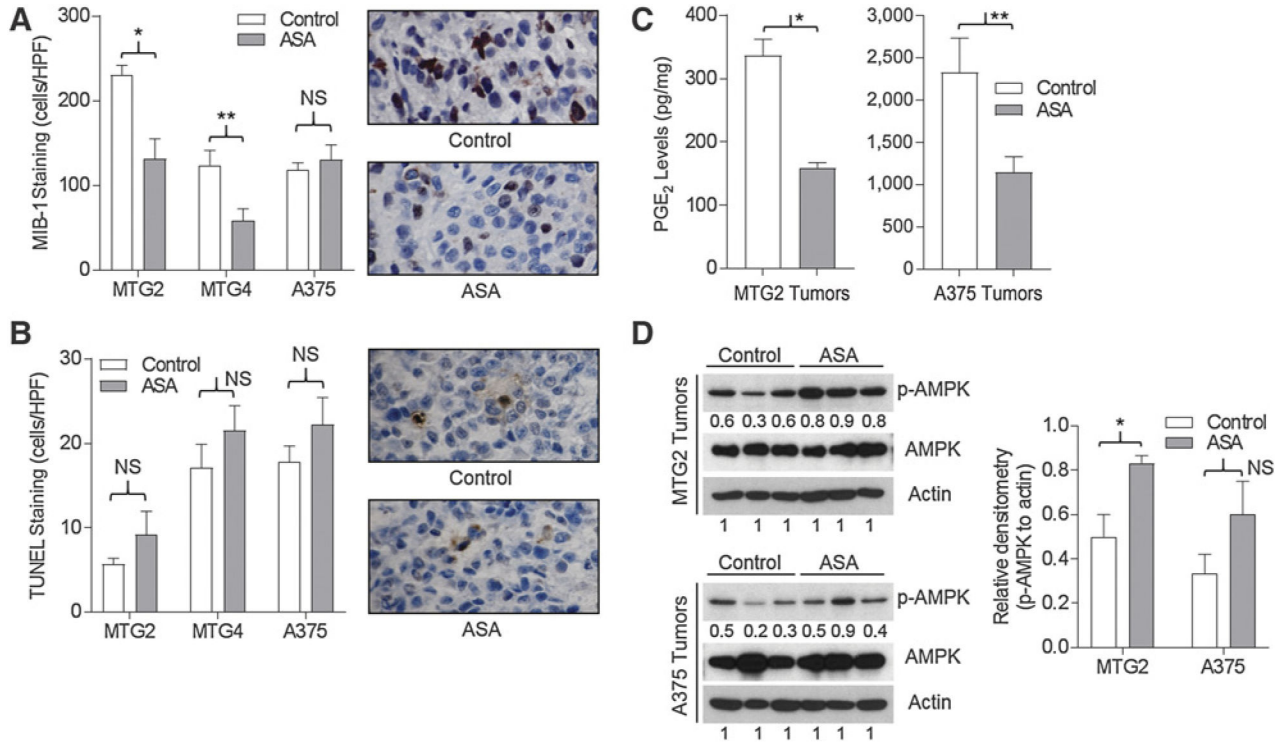
Figure 5.
Detection of salicylate and PGE_2 in mouse plasma and skin. Blood and skin were taken from mice ($n = 3–4$/group) not exposed to ASA (time 0) or 4 to 24 hours following a single oral dose of 0.4 mg ASA. **A,** Determination of salicylate (left) and PGE_2 (right) in plasma by LC/MS. *, $P = 0.01$; **, P 0.02; ***, $P = 0.03$. **B,** Determination of salicylate (left) and PGE_2 (right) in skin by LC/MS. *, $P = 0.005$; **, $P = 0.01$; ***, $P = 0.08$.
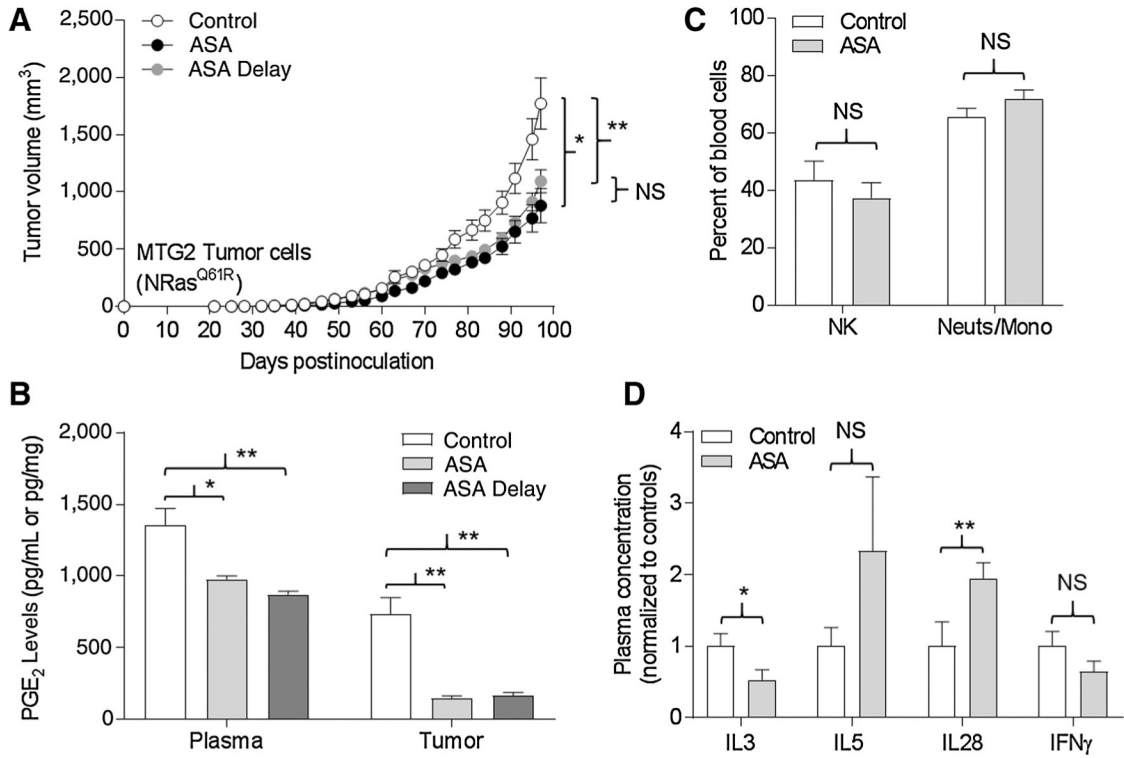
Figure 6.
ASA delays tumor growth of some cell implants. Daily oral gavage with 100 μL water (control) or ASA (0.4 mg) began one week prior to implantation of tumor cells or fragments (*n* = 10 mice/group), and continued daily until termination. **A,** Growth of MTG2 cells (left) and tumor fragments (right). *, *P* = 0.007; **, *P* = 0.08. **B,** Growth of MTG4 cells (left) and tumor fragments (right). *, *P* = 0.03; NS, not significant. **C,** Growth of A375 cells (left) and WM3311 cells (right).

Figure 7.
Proliferation, apoptosis, and signaling in ASA-sensitive and ASA-resistant tumors. Tumors were harvested from mice treated with daily water (control) or ASA gavage. **A,** MIB-1 staining cells per high-power field (HPF) from 4 to 5 tumors in each group. *, $P = 0.01$; **, $P = 0.02$; NS, not significant. Representative photos of MTG2 sections, ×400. **B,** TUNEL-positive cells per HPF from 4 to 5 tumors in each group. Representative photos of MTG2 sections, ×400. **C,** PGE_2 levels in tumors ($n = 3$ for each group). *, $P = 0.001$; **, $P = 0.05$. **D,** Western blotting of tumor lysates for p-AMPK, AMPK, and actin. Statistical analysis of densitometry values. *, $P = 0.03$.

Figure 8.
ASA inhibits growth and suppresses PGE$_2$ in established tumors. Oral daily gavage with 100 μL water (control) or ASA (0.4 mg) began one week prior to implantation of tumor cells, or with ASA (ASA delay) once tumors reached a diameter of 5 mm ($n = 9$–10 mice/group), and continued daily until termination. **A,** Tumor growth. *, $P = 0.004$; **, $P = 0.01$; NS, not significant. **B,** PGE$_2$ levels in plasma (pg/mL) and tumors (pg/mg) at termination. *, P 0.005; **, $P < 0.001$. **C,** Immune cell profiling of NK (DX5$^+$CD3$^-$) cells and neutrophils/monocyte (CD11b$^+$GR1$^-$) cells in blood at termination. **D,** Plasma cytokines at termination. Levels were normalized to the control group for each. *, $P = 0.03$; **, $P = 0.04$.